

Modelling a suspended nanotube oscillator

H. Üstünel*, D. Roundy and T. A. Arias

Department of Physics, Cornell University, Ithaca, NY 14853

*corresponding author: hande@physics.cornell.edu

We present a general study of oscillations in suspended one-dimensional elastic systems clamped at each end, exploring a wide range of slack (excess length) and downward external forces. Our results apply directly to recent experiments in nanotube and silicon nanowire oscillators. We find the behavior to simplify in three well-defined regimes which we present in a dimensionless phase diagram. The frequencies of vibration of such systems are found to be extremely sensitive to slack.

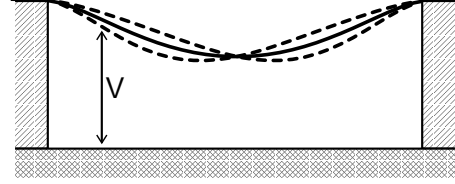
Vibrations of *one-dimensional* systems (i.e. systems with cross-sectional dimension much smaller than their length) suspended under the influence of a downward force have long been of interest in the context of such applications as beams, cables supporting suspension bridges and ship moorings [1, 2, 3]. Such systems display a wide range of behavior, depending on the amount of slack present in the system, the downward force, and the aspect ratio. Previous studies, which have largely been analytical, have been restricted to certain limiting cases of these parameters. Recently work on oscillating nanoscale systems, such as carbon nanotubes[4] and silicon nanowires[5], has opened the possibility of experimentally exploring such vibrations in entirely new regimes. In the present work, we study numerically the oscillations of a one dimensional elastic system over an extensive range of both the slack and force parameters, providing insight into the physics which separates this parameter space into three distinct regimes of behavior.

The treatment below is entirely general with illustrative examples taken from parameters relevant to carbon nanotubes. Since their discovery in 1991 [6], nanotubes have found many applications in device technology due to their small size, robust structure and superior elastic properties [7, 8, 9, 10]. Many of these applications involve the use of nanotubes as mechanical oscillators, making theoretical understanding of the vibrational properties of nanotubes in various geometries of current interest[4, 11]. Recent experiments [12] have studied the behavior of the transverse vibrations of a suspended nanotube clamped at both ends, under the action of a downward force, as sketched in Figure 1. These suspended nanotubes generally have around 1% *slack*, denoted in this work by s , which we define to be the ratio of the excess length of the tube to the distance between clamping points.

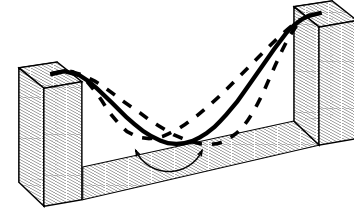
Analytic model and computational techniques — The potential energy of a one-dimensional elastic continuum under a uniform downward force is

$$\mathcal{U} = \frac{1}{2} \int_0^L \left[E u^2(l) + \frac{F}{R^2(l)} + f z(l) \right] dl \quad (1)$$

Here, l represents distance along the system of unstretched length L ; $u(l)$, $R(l)$ and $z(l)$ represent the local strain, radius of curvature and vertical displacement,



(a)



(b)

Figure 1. (a) Suspended nanotube under the action of a gate voltage V . (b) *Jump-rope* mode

respectively; E and F are the extensional and flexural rigidities; and f is the downward force per unit length. For single-walled nanotubes with diameters $d > 1$ nm, the rigidities we obtain using the Tersoff-Brenner empirical potential [13] are, to within 0.5%,

$$\begin{aligned} E &= 1.09 \cdot d & (\text{TPa} \cdot \text{nm}^2) \\ F &= Ed^2/8 = 0.14 \cdot d^3 & (\text{TPa} \cdot \text{nm}^4), \end{aligned} \quad (2)$$

regardless of the chirality of the tube [14]. We note that essentially the same values of E and F can be obtained using the in-plane elastic modulus of graphite.

To evaluate the potential energy (Equation 1), we begin with $\mathbf{r}(l)$, the *vector* location of the segment at position l from the end of the tube. The local strain is, then,

$$u(l) \equiv |\mathbf{r}'| - 1 \quad (3)$$

and inverse radius of curvature is

$$\frac{1}{R} \equiv \frac{|(1 - \hat{t}\hat{t})\mathbf{r}''|}{|\mathbf{r}'|^2}, \quad (4)$$

where prime indicates differentiation with respect to l , and the tangent vector $\hat{t} \equiv \mathbf{r}'/|\mathbf{r}'|$.

For a given force and slack, we discretize $\mathbf{r}(l)$ along l with a number of points (typically 30) sufficient to render all plots shown below visually indistinguishable under increasing resolution. To find the equilibrium configuration of the system under the action of the external force, we then relax the system using a conjugate gradients algorithm with forces computed using finite differences. Finally, we compute the force constant matrix $K_{ij} \equiv \frac{\partial^2 \mathcal{U}}{\partial x_i \partial x_j}$ and diagonalize it to obtain frequencies ν while assigning a mass $\mu \Delta l$ to each discretized point, where μ and Δl are the mass per unit length of the system and the distance between sample points respectively.

For a one-dimensional system, slack s , length L and downward force per unit length f can be regarded as *external parameters* that can be changed independently. Mass density μ and rigidities E and F on the other hand, all depend on the cross-sectional geometry of the system and can therefore be considered *internal parameters*. To make our discussion applicable to a general one-dimensional system, we present our results in units scaled by appropriate combinations of these basic parameters. In addition, we give results in physical units for the concrete system of a nanotube of diameter 2 nm with length $L = 1.75 \mu\text{m}$. For frequency plots, besides the physical frequency ν , we plot a dimensionless frequency $\tilde{\nu} \equiv \nu \sqrt{(\mu L^4/F)}$.

As a dimensionless measure of this force, we choose a *force control parameter* $\tilde{V} \equiv \sqrt{fL^3/F}$, proportional to the square root of the force. In recent experiments on suspended nanotubes[12], the external force was introduced via a gate voltage, as shown in Figure 3a. Such a voltage results in a force per unit length $f = \frac{1}{2} \frac{dc}{dz} V^2$. Here c is the capacitance per unit length of the nanotube given by

$$c = \frac{4\pi\epsilon_0}{2 \ln(z/d)}, \quad (5)$$

where ϵ_0 is the dielectric constant of vacuum and z is the distance between the wire and gate. For the concrete example of a $L=1.75\mu\text{m}$ nanotube with a diameter of 2nm, we take the tube to be suspended 500nm above the gate. In this case, a dimensionless parameter of $\tilde{V} = 10$ corresponds to a voltage of $\sim 4\text{V}$. As another example, a $100\mu\text{m}$ -long Si nanowire of 100nm diameter, with a z of $25\mu\text{m}$ would require a voltage of $\sim 60\text{V}$ to attain the same force control parameter \tilde{V} of ten. Moving to larger systems, a 0.6mm-diameter steel piano wire which is $\sim 2\text{m}$ long under the influence of gravity would have the same dimensionless parameter of $\tilde{V} = 10$.

Figures 2 and 3 display our primary results, both in dimensionless form and for the nanotube example, for the dependence of the vibrational frequency on slack and force. Figure 2 shows the dependence of frequency on slack over the range of small slacks for zero force.

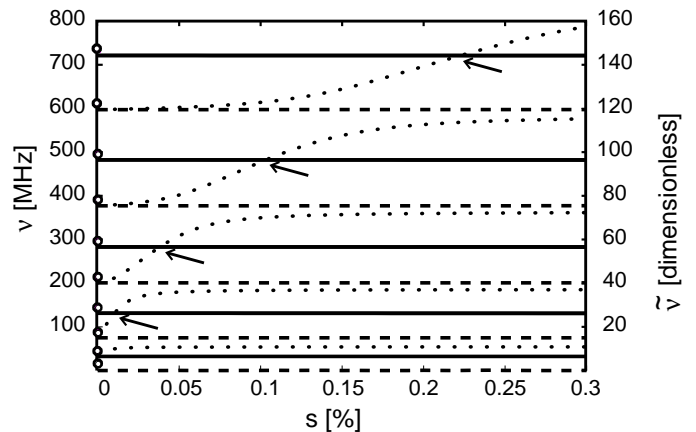
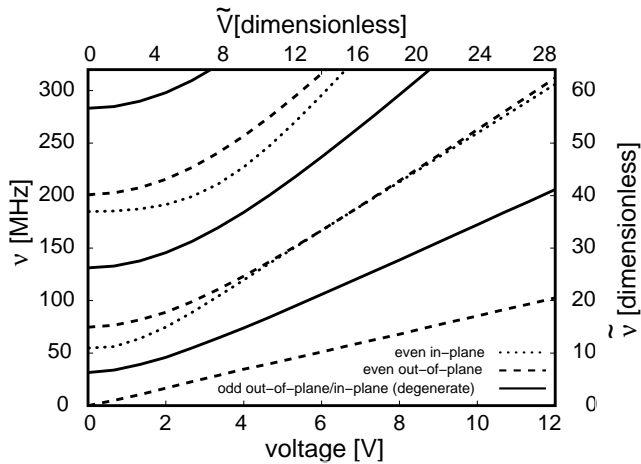


Figure 2. Frequency versus slack at zero force control parameter: classic solution for zero slack (points on vertical axis), numerical results for non-zero slack (curves). The dimensionless frequency $\tilde{\nu} = \nu \sqrt{\mu L^4/F}$ applies to a general system. The modes are doubly-degenerate and odd (solid curves), out-of-plane and even (dashed curves) or in-plane and even (dotted curves). Arrows indicate mode crossings.

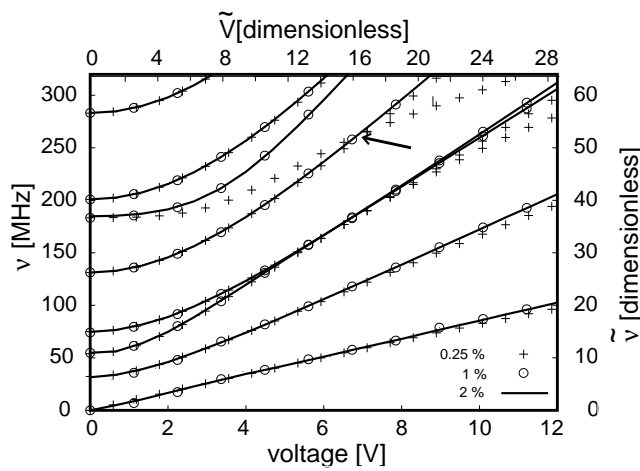
The style of the curves indicate whether the mode is doubly-degenerate and odd (solid), out-of-plane and even (dashed) or in-plane and even (dotted). After the mode crossings shown with arrows in Figure 2, all curves remain flat up through a slack of 2%, the largest slack considered in this paper. Figure 3 shows the dependence of the frequency on the force control parameter. Figure 3(a) shows the symmetry of the modes as in Figure 2 for a system of 1% slack. Figure 3(b) shows slacks of $s=0.25\%$, 1% and 2% with the horizontal axis scaled by $\sqrt[4]{s}$ which, for reasons described below, causes the curves to collapse upon each other for all but the smallest slack.

We find three simplifying limits for the physical behavior of the system as a function of slack s and force control parameter v . In each such limit, a different term in the potential energy (Equation 1) dominates with the other terms either being negligible or acting as a constraint. These three regimes, which we term *buckled beam*, *hanging chain* and *hanging spring*, are shown in Figure 4.

For small external forces, the extensional rigidity acts as a constraint which keeps the tube length fixed. If the force is sufficiently small, the bending term in Equation 1 dominates the dynamics and the system acts like an *Euler-buckled beam*. The *in-plane* vibrations of buckled beams have been studied analytically, but only in the absence of an applied force and only under conditions of very small slack (under $\sim 0.07\%$ [2]). Our results extend this treatment to three dimensions and larger values of slack, probing at the same time the dependence on the downward force. In the absence of applied force all modes are doubly degenerate at zero slack with the frequencies



(a)



(b)

Figure 3. (a) Dimensionless frequency versus force control parameter: in-plane modes (dashed curves), out-of-plane modes (dotted curves), degeneracy of in- and out-of-plane modes (solid curves). (b) Dimensionless frequency versus force control parameter scaled by fourth-root of slack ($\nu/\sqrt[4]{s/1\%}$) for three values of slack s : 0.25% ('+'), 1% ('o'), 2% ('⊙'). Frequency in MHz and voltage in V refer to the nanotube example described in the text. The scaled frequency $\tilde{\nu} = \nu\sqrt{\mu L^4/F}$ and the force control parameter $\tilde{v} = \sqrt{fL^3/F}$ apply to a general system.

of the classic unbuckled clamped beam [15], shown as circles on the vertical axis of Figure 2.

With the introduction of slack, the lowest out-of-plane mode, which we term “jump rope”, corresponds to rotation of the relaxed system about the clamping points, as illustrated in Figure 1b. Rotational symmetry requires that this mode has zero frequency in the absence of an external force. It therefore shows up as a dashed line

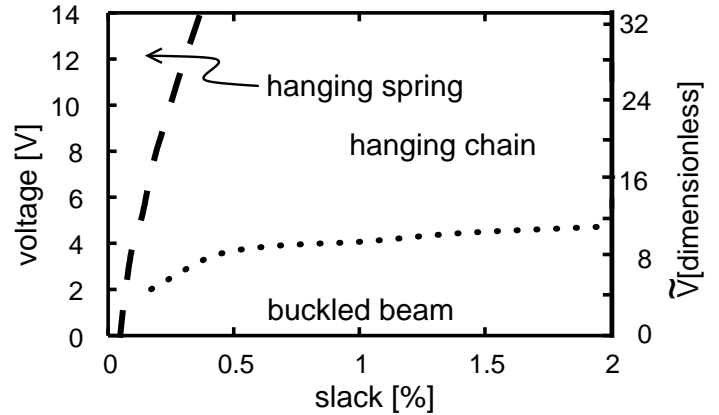


Figure 4. The three regimes in which nanotube behavior simplifies, as a function of voltage and slack. The dashed line between the “hanging spring” and “hanging chain” regimes is the crossing between the second even in-plane mode and the second odd in-plane mode. The dotted line separating the “buckled beam” regime from the “hanging chain” regime is the contour on which the derivative $\frac{d \log \omega}{d \log s}$ has a value of $-1/8$. The axis on the right shows the force control parameter,

$$\tilde{V} = \sqrt{fL^3/F}$$

overlying the slack axis of Figure 2. No such symmetry applies to other out-of-plane modes, whose frequencies drop slightly, and then remain essentially independent of slack.

In contrast to the out-of-plane modes, the in-plane modes are affected by a length-conservation constraint which changes with the amount of slack. For reasonably small slack, the odd modes (shown as solid lines) are unaffected by this constraint, since they conserve length by symmetry, and thus remain degenerate with their out-of-plane counterparts. The even modes (shown as dotted lines), in order to conserve the tube length, acquire two extra nodes as slack is introduced, leading to a mode crossing between the even and odd modes (shown with arrows in Figure 2).

When the force is large enough to overcome the bending term in Equation 1 but still too small to stretch the nanotube, the tube behaves as a *hanging chain* clamped at both ends, whose equilibrium profile forms the well-known *catenary*. In this regime, the slack dependence of the frequency can be solved for analytically in the limit of small slack. In the small slack limit, the shape of the tube is parabolic, and the tension is constant throughout the tube. The frequency is then determined by the result

for a simple string under tension, giving

$$\omega_n = n\pi \sqrt{\frac{f}{\mu L \sqrt{24s}}} \quad (6)$$

Since in this equation the frequency is proportional to $s^{-1/4}$, we scale the horizontal axis in Figure 3(b) by $\sqrt[4]{s}$, causing the curves for each slack value to collapse for small forces, although for 0.25% slack there is deviation in the higher modes, in particular in the mode pointed to by the arrow.

For a given force, as the slack decreases, the tension increases and eventually the tube begins to stretch and departs from the hanging chain regime. This avoids the infinite frequency at very small slack which is predicted by Equation 6. This effect is responsible for the deviation from linear behavior of the tube with 0.25% slack in Figure 3, in contrast to the tubes with 1% and 2% slack.

In the large force, small slack regime, the extensional term in Equation 1 can no longer be treated as a constraint, as the tube begins to stretch. The nanotube then behaves as a *hanging spring* clamped at both ends. The frequency in this regime can be derived in a manner similar to that in the hanging chain regime: the shape of the nanotube is parabolic and the tension is constant throughout the tube. However, in the case of the hanging spring, the tension is proportional to the change in length of the tube. Under these conditions, the frequency is proportional to the cube root of the force:

$$\omega_n = n\pi \left(\frac{5}{3}\right)^{1/3} \sqrt{\frac{(EL)^{1/3}}{6\mu L}} f^{1/3} \quad (7)$$

The frequency is independent of slack, because as the tube is stretched the original amount of slack in the nanotube becomes insignificant. However, the point of onset of the hanging spring regime does depend on slack.

In the buckled beam and hanging chain regimes, the length conservation constraint in a slack tube forces the first even in-plane mode to have two nodes. In contrast, in the hanging spring regime there is no length conservation constraint, and consequently, the lowest frequency in-plane mode has no nodes. As the transition between these regimes occurs, there is a mode crossing between the even and odd in-plane modes, shown with an arrow in Figure 3 in the curve for 0.25% slack. The crossing between the second even in-plane mode and the second odd in-plane mode is shown as the dashed curve in Figure 4 which separates the hanging spring regime from the hanging chain regime.

In conclusion, we have studied numerically and analytically, as a function of both the amount of slack and applied force, the transverse vibration frequencies of one dimensional suspended systems clamped at both ends.

We have chosen as a concrete application to focus on suspended nanotubes under the influence of a gate voltage which have recently been studied experimentally [12]. We find three regimes in which the behavior simplifies and can be understood using approximate analytic solutions. This understanding is important in characterizing and designing nanoresonators where it can prove difficult to control or measure parameters such as slack. The hanging chain regime is particularly suitable for tuning and characterizing nano-oscillators, since Equation 6, which governs the frequency in this regime, remains valid independently of imperfections affecting the boundary conditions at the clamps.

This work was supported by the NSF through the Cornell Center for Materials Research and the NIRT program.

References and Notes

- [1] H. M. Irvine and T. K. Caughey, Proc. R. Soc. London, Ser. A **341**, 299 (1974).
- [2] A. H. Nayfeh and W. Kreider, AIAA Journal **33**, 1121 (1995).
- [3] N. Kitney and D. T. Brown, Journal of Offshore Mechanics and Arctic Engineering **123**, 1 (2001).
- [4] S. Sapmaz, Y. M. Blanter, L. Gurevich, and H. S. J. van der Zant, PRB **67**, 235414 (2003).
- [5] D. W. Carr *et al.*, Appl. Phys. Lett. **75**, 920 (1999).
- [6] S. Iijima, Nature **354**, 56 (1991).
- [7] R. M. D. Stevens *et al.*, Nanotechnology **11**, 1 (2000).
- [8] K. Keren *et al.*, Science **302**, 1380 (2003).
- [9] T. Shimada *et al.*, Appl. Phys. Lett. **84**, 2412 (2004).
- [10] W. Yang *et al.*, Nature Materials **1**, 253 (2002).
- [11] M. Dequesnes, S. V. Rotkin, and N. R. Aluru, Nanotechnology **13**, 120 (2002).
- [12] V. Sazonova *et al.*, Nature **431**, 284 (2004).
- [13] D. W. Brenner, PRB **42**, 9458 (1990).
- [14] J. P. Lu, Phys. Rev. Lett. **79**, 1297 (1997).
- [15] L. D. Landau and E. M. Lifshitz, *Theory of Elasticity* (Pergamon Press, New York, 1970), p. 116.